

Persistence Length of Isotactic Poly(hydroxy butyrate)

G. Beaucage,* S. Rane, and S. Sukumaran

Department of Materials Science and Engineering, University of Cincinnati, Cincinnati, Ohio 45221

M. M. Satkowski and L. A. Schechtman

Miami Valley Laboratories, Procter & Gamble Corporation, P.O. Box 538707, Cincinnati, Ohio 45253-8707

Y. Doi

*The Institute of Physics and Chemistry Research (RIKEN), 2-1 Hirosawa, Wakoshi, Saitama 351-01, Japan**Received March 18, 1997; Revised Manuscript Received May 2, 1997*

ABSTRACT: The persistence length of isotactic poly(hydroxy butyrate) was measured using small-angle neutron scattering. The value obtained from these measurements reflects a high degree of local chain persistence. If this local persistence is accounted for, scattering from these chains can be globally fit with Gaussian scaling. A global scattering function, the unified equation, is used, which decomposes the chain structure into two levels, one corresponding to the Gaussian regime and one to the persistence regime. The persistence length obtained using this global scattering function is compared to that obtained using the graphical approach of Kratky and Porod with good agreement. Additionally, the global fitting approach of Sharp and Bloomfield is also considered. The Kratky and the Sharp and Bloomfield approaches appear to yield different values for the persistence length. Additionally, the Sharp and Bloomfield function does not allow inspection of the component parts of the fit. One advantage of both global functions is that the level of statistical confidence in the persistence length can be determined in a least-squares fit. Another advantage is the removal of ambiguity concerning an apparent regime of non-Gaussian scaling between the persistence scaling regime and the Gaussian regime.

Introduction

Isotactic poly(hydroxy butyrate), i-PHB, is a biosource polyester which is thought to have extended local chain conformations in the melt and in the amorphous state. This is reflected by unusual melt rheology¹ among other physical properties.^{2,3} Because rheology is effected by the local persistence of the chains, a measure of this persistence is desired in order to understand the processibility of these biosource polyesters. It is expected that chains with large persistence units will follow the Kratky/Porod model for a persistent chain^{4,5} and may be useful for a comparison of different approaches to the analysis of scattering data from persistent chains. In the Kratky and Porod model,^{4,5} the chain is composed of average linear segments of some length, l_K , and some cross-sectional area A_K . l_K is the Kuhn-step length following the model of Kuhn, first introduced in 1934,⁶ and $l_K = 2l_p$ ⁷ where l_p is the persistence length which can be observed in a static scattering experiment, as discussed below. A_K is described by a two-dimensionally-averaged, cross-sectional radius of gyration, R_c , orthogonal to the chain's contour length. The contour length, L , follows the end points of the Kuhn units, $L = n_K l_K$, where n_K is the number of Kuhn units in the chain. In a Gaussian chain these basic physical units build an object of mass-fractal dimension, $d_f = 2$, such that the average end-to-end distance for the chain, R_{eted} , is given by $n_K^{1/d_f} l_K$. In non-Gaussian chains, d_f may vary from 2; for example, in a semi-dilute, good solvent d_f is thought to be approximately $5/3$ between the persistence length and the size of a blob.^{8,9} Between the size of a blob and the chain's radius of gyration, R_g , the scaling is Gaussian for semidilute, good-solvent conditions, and d_f theoretically shows a transition to 2. For dilute-

solution, good-solvent conditions the blob size is the same as the chain's R_g and the chain displays only expanded scaling with $d_f \approx 5/3$. Such deviatory scaling behavior has never been conclusively demonstrated by direct fitting of SANS data. The approach, presented here, offers some hope at demonstrating these features directly in a SANS experiment, although they do not appear to apply to PHB melts.

The persistence length, l_p , was introduced by Kratky and Porod^{4,5} as a direct measure of the average local conformation for a linear polymer chain. The persistence length reflects the sum of the average projections of all chain segments on a direction described by a given segment. Kratky^{10–12} described the features of the persistence length, l_p , in a small-angle scattering pattern; in particular, a regime of dimension 1 in the small-angle scattering pattern corresponds to Kratky and Porod's definition of the persistence unit. The mass-fractal dimension of an object can be directly determined in a scattering pattern through the application of mass-fractal power-laws.¹³ Using these laws, an object of mass-fractal dimension d_f displays a power-law described by, $I(q) = Bq^{-d_f}$, for $1 \leq d_f < 3$. A power-law of -2 is expected for the Gaussian regime and a power-law of -1 for the persistence regime. In order to resolve the persistence length, l_p , a log-log plot of $I(q)$ versus q can be made and the two power-law regimes matched with lines of slopes -2 and -1 ; cf. Figure 1. The intersection of these two lines in q is related to the persistence length through $6/(\pi q_{\text{intersection}}) = l_p$ (see ref 10, p 363). q is the absolute value of the momentum transfer vector, $q = 4(\pi/\lambda) \sin(\theta/2)$, λ is the wavelength of the scattered radiation and θ is the scattering angle. (Equivalently, a "Kratky plot" of Iq^2 vs. q can be made to account for Gaussian scaling, and the deviation from a horizontal line can then be used to estimate l_p .) This

* Abstract published in *Advance ACS Abstracts*, June 15, 1997.

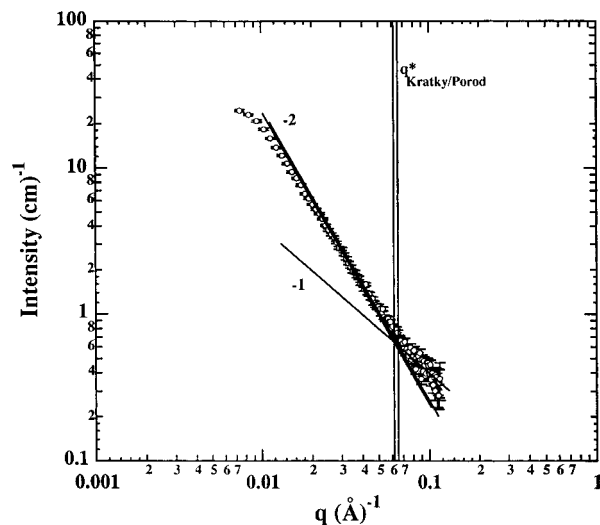


Figure 1. Kratky/Porod graphical analysis in a log-log plot of corrected SANS data from a 5% by volume d-PHB sample in h-PHB. The lower power -2 line is the best visual estimate; the upper line is shifted to match the unified fit (using (3)) of Figure 2. Key: left, q^* corresponds to best visual estimate; right, plot to match unified fit of Figure 2. The statistical error in the data is shown.

approach has been summarized in several reviews (see refs 10 and 14 (Appendix G, p 401).

The statistical segment length, l_{ssl} , is a related parameter defined as the scaling factor between the chain's radius of gyration, R_g , and the square root of the number of chemical mer units in the chain, n_{chem} , where $R_g = 2l_{\text{ssl}}(n_{\text{chem}}/6)^{1/2}$. For a freely-jointed, Gaussian chain, where the Kuhn unit is a chemical mer unit, $2l_{\text{ssl}} = l_K = 2l_p$ and $n_K = n_{\text{chem}}$. The specific definitions of these terms becomes important for chains with bond restrictions where $n_K \neq n_{\text{chem}}$ and $2l_{\text{ssl}} \neq l_K$, that is, the Kuhn segment and the persistence length are both independently-measurable, physical parameters while, in most cases, the statistical segment length is an arbitrary parameter which depends on the chemical definition of a chain unit. In general, $l_K = 2l_p$.⁷⁻⁹ When the global chain scaling deviates from Gaussian, such as in good and poor solvents, the statistical-segment length refers to an *equivalent-Gaussian chain* which does not physically exist. Even under these deviatory scaling conditions, there remains a scaling relationship between l_{ssl} and l_K ,¹⁵ and the persistence length and Kuhn-step length retain their physical definitions.

Although the definition of the persistence length by Kratky and Porod^{4,5} appears to be somewhat vague in terms of real space, it is the only physical parameter that can be independently determined that directly reflects local chain conformation at thermodynamic equilibrium. Because of this, the persistence length is a focus of calculations of chain conformation using chemical bond lengths and angles.^{10,14,16} In the more complicated chemical structures, seen in biology for instance, such calculations become tedious and are subject to some degree of uncertainty due to the dominance of secondary chain architecture. In fact there has been little experimental verification of *ab initio* calculations of the persistence length for polymers more complicated than monosubstituted vinyl polymers. The issue becomes complicated when chain secondary structures such as tacticity and helical coiling become important to chain conformation.¹⁷⁻²² A direct measure of the persistence length using small-angle scattering remains the most robust approach to describing local chain conformations. A combination of the Kratky-

Porod approach with modern scattering functions and an understanding of fractal scaling laws offer hope in describing both chain conformation as well as the statistical thermodynamics of these complicated systems.¹⁵

Sharp and Bloomfield Global Function

The graphical approach of Kratky and Porod^{5,6,10,11} for the determination of the persistence length is subject to some ambiguities. Rather than a discrete transition regime between power-law -2 scaling (Gaussian coil) and power-law -1 scaling (rodlike, persistence), all polymers display a gradual transition. Some equations are available to describe this transition regime, the most widely used being that of Sharp and Bloomfield²³ as corrected by Schmidt²⁴

$$I(q) = G_2 \left\{ g_D(x) + \frac{2l_p}{L} \left[\frac{4}{15} + \frac{7}{15x} - \left(\frac{11}{15} + \frac{7}{15x} \right) e^{-x} \right] \right\} \quad (1)$$

where $g_D(x)$ is the Debye scattering function for a Gaussian chain²⁵

$$g_D(x) = 2 \frac{e^{-x} + x - 1}{x^2} \quad (2)$$

x is equal to $(Ll_p q^2)/3$, L is the contour length, $2l_p n_K$, and G_2 in (1) is the Guinier or Debye prefactor. For isolated chains, $G_2 = N_{\text{chain}} n_{\text{chain}}^2$, where N_{chain} is the number of chains in the scattering volume for dilute concentrations and n_{chain} is a contrast factor between the chain and the solvent.²⁶ For higher concentrations a factor of $\phi_v(1 - \phi_v)$ can be used²⁶ for polymer/solvent systems. For the determination of structural sizes such as the persistence length and the chain's radius of gyration, absolute units for intensity are not necessary in a scattering experiment since these parameters are determined by the values of q and the relative shape of $I(q)$.

The Sharp and Bloomfield function, eq 1, is sufficient for the description of a transition between Gaussian and rodlike scattering at the persistence length. In spite of this success, several improvements are possible using more recent scattering functions, described below. Although eq 1 accounts for the persistence regime, the rodlike scattering regime (power-law -1) of the persistence unit is not independently defined in (1). Generally, (1) is only good up to $q < 2/l_p$ (cf. Figure 3). This means that (1) is only useful for q values approaching the transition region where the coil scaling goes from -2 to -1 power-law slope. Additionally, (1) is not flexible enough to account for deviations from Gaussian scaling, although some attempts at extending equation (1) have been made.²⁷ Because of these limitations, a global function, which could describe the persistence regime in a more complete fashion, is desirable.

Unified Function

Recently, an approach which describes small-angle scattering in terms of arbitrary levels of structure has been presented.²⁸⁻³⁰ This global approach has proven useful in describing mass-fractal systems.³¹⁻³⁴ A major contribution of this approach is in describing the transition regime between structural levels in small-angle scattering. Of interest here is the transition regime between persistence scaling, $d_f = 1$, and the Gaussian, $d_f = 2$, or mass-fractal regime for global scaling of a polymer coil.

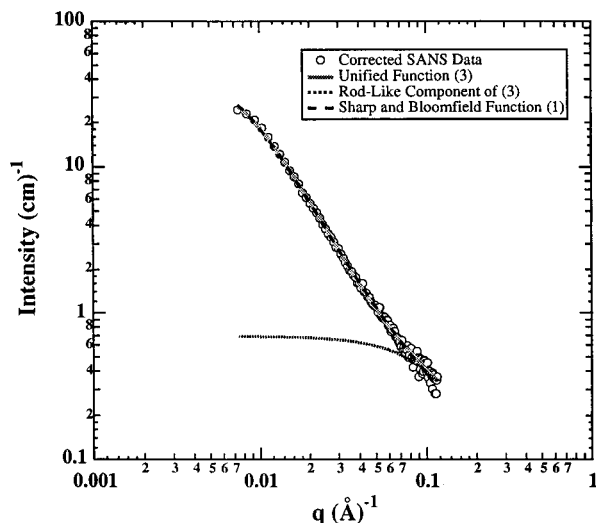


Figure 2. Unified (eq 3) and Sharp and Bloomfield (eq 1) fits to the corrected data of Figure 1 (the two fits overlap in this plot). Fit parameters are given in the text. The fit range includes all of the data points shown.

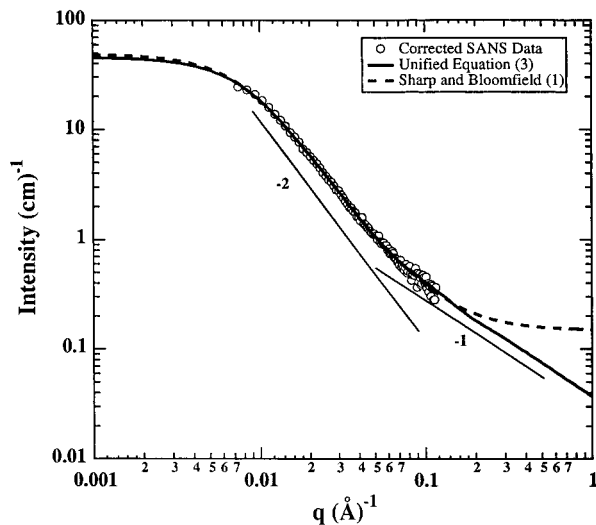


Figure 3. Extrapolations of the fits of Figure 2 showing deviation of Sharp and Bloomfield and unified approaches at high- q . Equation 3 can be easily extended to describe the cross-sectional radius of the persistence unit if data pertaining to the high- q regime were available, eq 3'.

In the unified approach, small-angle scattering is described by a structurally-limited summation of scattering laws from each level of structure. A level of structure corresponds to a Guinier regime and a structurally-limited power-law regime. It is the structural limits to the power-law regimes that describe the overlap of structural levels.^{28–30} The unified function, as applied to the two structural levels of a Kratky/Porod persistent chain, is given by

$$I(q) = \{ G_2 e^{-(q^2 R_{g2}^2)/3} + B_2 e^{-q^2 l_p^2/3} (q_2^*)^{-2} \} + \{ G_1 e^{-(q^2 R_{g1}^2)/3} + B_1 (q_1^*)^{-1} \} \quad (3)$$

where

$$q_i^* = \left[\frac{q}{\{\text{erf}(qkR_{g_i}/\sqrt{6})\}^3} \right] \quad (4)$$

and $k \approx 1.06$. In (3) the two terms in braces refer to the Gaussian scaling regime, first brackets and subscript "2", and persistent rodlike scaling regime, second

brackets and subscript "1". In each set of braces, the first term describes a Guinier exponential decay (a knee in a log–log plot, cf. Figure 3). The second term in each of the brackets describes a structurally-limited power law. The exponential term in the second term of the first set of brackets describes the high- q limit for Gaussian scaling at l_p ,³⁵ while (4) describes the low- q limit at R_{g_i} .

In (3), G_2 is the Gaussian prefactor for the Debye–Gaussian regime described above. R_{g2} is the coil's radius of gyration. For a Gaussian chain

$$(R_{g2,\text{Gaussian}})^2 = \frac{n_K (2l_p)^2}{6} \quad (5)$$

and for arbitrary mass-fractal scaling^{28,30}

$$R_{g2}^2 = \frac{n_K^{2/d_f} (2l_p)^2}{(1 + 2/d_f)(2 + 2/d_f)} \quad (6)$$

For Gaussian scaling, B_2 is given by

$$B_{2,\text{Gaussian}} = \frac{2G_2}{R_{g2}^2} \quad (7)$$

and for arbitrary mass-fractal scaling,^{28,30}

$$B_2 = \frac{d_{f2} G_2}{R_{g2}^{d_{f2}}} \Gamma(d_{f2}/2) \quad (8)$$

and the power -2 in the first set of braces of eq 3 is replaced by a power $-d_{f2}$. Equations 3–8 can be used to account for good solvent scaling, for instance, if the power-law of -2 in eq 3 is replaced with a power-law of $-5/3$.

G_1 in (3) is G_2/n_K (see ref 11, pp 192–193). R_{g1} is defined for an infinitely thin rod of length $l_K = 2l_p$, as (see ref 11, p 69)

$$R_{g1} = \frac{l_p}{\sqrt{3}} \quad (9)$$

Equation 9 ignores the cross-sectional dimension of the chain, R_c , as discussed below. B_1 is defined for a rod as (see refs 11 (p 192), 24 (p 27), and 34–36)

$$B_1 = \frac{\pi G_1}{2l_p} \quad (10)$$

(3), with the constraints of (6)–(10), defines the scattering from a persistent, Gaussian chain in terms of three parameters, a contrast/concentration factor, G_2 , the persistence length, l_p , and the number of Kuhn segments, n_K . Additionally, non-Gaussian, persistent chains can be described using the mass-fractal dimension, d_{f2} , as an additional fitting parameter, such as in good solvent conditions.

It should be noted that the degree of polymerization in terms of the number of Kuhn units, n_K , corresponds to the value which should be used to calculate statistical thermodynamic parameters using the Flory lattice model³⁹ since this reflects the actual number of physical units in the chain. This is consistent with the idea that the number and size of the persistence units does not change with solvent conditions.^{14,38} (In fact, this has no effect on the calculation of the entropy of mixing for Gaussian chains but leads to a significant error when non-Gaussian scaling is considered.^{15,40})

l_p is probably somewhat overestimated in eq 9 since the cross-sectional radius of the persistence units has been ignored in (9). This can be corrected if an estimate of the chains cross-sectional radius can be made either from scattering data or from models for the molecular structure

$$R_{g1} = \sqrt{\frac{l_p^2}{3} + \frac{R_c^2}{2}} \quad (9)$$

It is possible to include the radius of the persistent units in the unified function as a third level of structure,²⁸⁻³⁰ if a sufficient q range were available

$$I(q) = \{G_2 e^{-(q^2 R_{g2}^2)/3} + B_2 e^{-q^2 l_p^2/3} (q_2^*)^{-2}\} + \\ \{G_1 e^{-(q^2 R_{g1}^2)/3} + B_1 e^{-q^2 R_c^2/3} (q_1^*)^{-1}\} + \\ \{G_1 e^{-q^2 R_c^2/3} + B_1 (q_1^*)^{-4}\} \quad (3')$$

where B_1 is defined by Porod's Law for a rod structure of length $2l_p$ and radius R_c , and G_1 , as discussed in ref 28, is given by

$$G_1 = G_1 \left(\frac{R_c}{2l_p} \right)^2 \quad (11)$$

Equations 1-11 are sufficient for polymer/solvent systems with G_2 being replaced by $\phi(1 - \phi)G_2$ for higher concentrations. For blends of deuterated and hydrogenous polymers the RPA equation is usually used⁹

$$\frac{1}{I(q)} \approx \frac{1}{k_d P_d(q)} + \frac{1}{k_h P_h(q)} - 2\chi \quad (12)$$

where only the scaling behavior is shown, which is sufficient for determination of molecular sizes. $P(q)$ for each of the two components is given by either the Sharp and Bloomfield model, eq 1 or the unified function, eq 3. Under the assumption that the interaction parameter, χ , is negligible, and only effects the scattered intensity at low q , and that $P_d(q) \approx P_h(q)$, especially at high- q , then eqs 1-11 are sufficient to describe scattering, especially at high- q , for polymer/polymer, amorphous, isotopic systems in the miscible regime. Similarly, the effect of polydispersity will dominate at low- q in the region of the radius of gyration and is not an important issue at high- q in the regime where the local chain persistence is observed.¹²

Experimental Section

Deuterated isotactic PHB was obtained by microbial synthesis using deuterated feed stock as reported elsewhere,^{2,3,41} while hydrogenous atactic PHB was obtained by synthetic polymerization.^{2,3,42} Both PHB's chemical degrees of polymerization are close to 1000. The polydispersity of these samples is fairly high, ≈ 2 , and moreover, some degradation is known to occur at temperatures above the melting point, ca. 130 °C, on extended exposure. Because of the uncertainty in the chemical degree of polymerization, R_g for the coils was used as a fitting parameter using eq 5 in eqs 1 and 3.

A low concentration of deuterated isotactic-PHB, 5 vol %, was prepared by solution blending in chloroform at a total polymer concentration of 10%. This was precipitated from solution using methanol and vacuum dried at 70 °C for several days. Plaques of the blends were prepared by melt pressing into 2 mm thick by 1.5 cm diameter samples for the neutron-scattering experiment. Similar plaques were prepared for the purely hydrogenous and purely deuterated samples. All of the samples were heated above the melting point for PHB (≈ 130 °C) for 4 min followed by quenching in a methanol/dry ice bath. This produced largely amorphous samples for the

neutron-scattering experiment as verified in separate experiments using optical birefringence, DSC, and SAXS.

Neutron scattering was performed at the National Institute of Standards and Technology on the 8 m SANS beam line with the detector offset to expand the available q range. A standard brass cell was used with thin aluminum windows. An empty cell run was subtracted from all data. Standard data correction procedures were followed, which include measurement of transmissions and correction for the empty cell, detector sensitivity and dark current as well as azimuthal averaging to obtain $I(q)$ vs. q in absolute units of cm^{-1} . Samples were held in a cryostat at -20 °C during the run to retain the quenched, amorphous state. Incoherent scattering from the purely hydrogenous and purely deuterated samples was weighted by the sample composition and subtracted from the data to yield the incoherently corrected scattering pattern, shown in Figure 1. Statistical errors were propagated from the number of counts through all corrections.

Determination of l_p for PHB. The corrected SANS data and propagated statistical error for a 5% isotactic d-PHB blend is shown in the log-log plot of Figure 1. The lines of slope -2 and slope -1 indicate the two scaling regimes for the globally Gaussian chains and the local, rodlike persistent units. The vertical line indicates the intersection of the two power laws at $q^* = 0.0614 \text{ \AA}^{-1}$. Using $l_p = 6/(\pi q^*)$,^{4,5,10,11} this corresponds to $l_p = 31.1 \pm 3.5 \text{ \AA}$. This value includes an error estimated from the qualitative nature of matching the lines of slope -2 and -1 to the data. Local power-law fits do not significantly change this error since the power -2 regime is extremely sensitive to the fit range. In addition to the error involved in this estimation of the persistence length, it is not clear from an inspection of the data that the assumption of Gaussian scaling is correct, i.e. the power-law -2 regime. In fact, a line of slope $-5/3$ will fit the data in the crossover regime ($\approx 0.04\text{--}0.085 \text{ \AA}^{-1}$). As noted above, a slope of $-5/3$ has a physical interpretation related to a semidilute, good-solvent condition as discussed above. Because of this and because of the large error inherent in the graphical approach of Figure 1, it is desirable to fit the entire scattering curve using a global approach such as (1) or (3).

A least-squares fit to the data of Figure 1 using eqs 1 and 3 was performed; see Figure 2. The fits of (1) and (3) are virtually indistinguishable in Figure 2. The fit parameters for the unified fit as well as the statistical errors are as follows: $G_2 = 45.3 \pm 1 \text{ cm}^{-1}$; $l_p = 29.2 \pm 0.4 \text{ \AA}$; $n_K = 66 \pm 2$. For (1) the parameters are $G_2 = 49.1 \pm 1 \text{ cm}^{-1}$, $l_p = 26.4 \pm 0.5 \text{ \AA}$, and $n_K = 89 \pm 3$. If the Sharp and Bloomfield value for l_p is used in Figure 1, q^* will occur at 0.072 \AA^{-1} , which is not reasonable using the Kratky/Porod graphical approach.

Figure 2 also shows the second bracketed term of (3) independently plotted. This curve corresponds to the component of the unified fit for the rodlike persistence units. A similar plot is not possible for (1). This curve serves as a check of the reasonableness of the fit parameters. One advantage of the global functions is that the overlap regime close to the persistence regime is described in both fits and is included in reduction of the statistical error for the three fit parameters. The apparent deviations from Gaussian scaling, in Figure 1, at low- q , and in the overlap regime are shown to be a manifestation of the Debye function at low q , $g_D(q)$ in (1), and the overlap regime at high- q , in Figure 2.

As noted above, the Sharp and Bloomfield function (1) is usually restricted to values of q below $2/l_p$ (ref 11, p 193). The unified function, eq 3, is limited to the structural model which has been used for the data fit. In this case, this limits the fit to q values where the persistence cross sectional radius can not be observed (on the order of 0.3 \AA^{-1} for this case). Figure 3 shows high- and low- q extrapolations of the fits of Figure 2 which demonstrate these limitations. Equation 3 can be easily extended to the radial features of the persistent unit, (3') above, if such features were observed in the scattering. This would be manifested as a Guinier-knee²⁸⁻³⁴ at high- q in the log-log plot, followed by a Porod regime of -4 slope at highest q , eq 3', reflecting the surface to volume ratio for the persistent units. Additionally, structural features related to helical coiling and other secondary structures can be easily incorporated in the unified approach. Inclusion of these features requires a model for these additional levels of structure.

Characteristic Ratio. The persistence length and number of Kuhn segments can be used to calculate several molecular parameters for isotactic PHB. Using the values from the unified fit in (3), the chain contour length, L , is $3,830 \pm 170$ Å, the end-to-end distance, R_{eted} , is 473 ± 13 Å, and the radius of gyration, R_g , is 193 ± 5 Å. The characteristic ratio ref 14, Appendix G), C_∞ , is given by

$$C_\infty = \left(\frac{2l_p}{l_{\text{chem}}} \right) - 1 = 39.1 \pm 0.5 \quad (13)$$

where $l_{\text{chem}} = 1.455$ Å is the square root of the mean of the square of the four bonds comprising the main chain repeat unit (ref 14, pp 183 and 188). Since the usual value for C_∞ is 5–12,^{14,36} this reflects a large degree of local persistence in isotactic PHB.

Conclusion

The persistence length for PHB was determined directly from SANS data using three approaches, the Kratky/Porod approach (31.1 ± 3.5 Å), the Sharp and Bloomfield function (26.4 ± 0.5 Å), and the unified function (29.2 ± 0.4 Å). The value obtained from the unified function is reasonable in that a Kratky/Porod construction can be made for this value in agreement with the data (Figure 1) and the high- q , rodlike component of the fit can be isolated and compares reasonably with the data (Figure 2). The Sharp and Bloomfield function, (1), seems to underestimate the persistence length in the global fit. It is more difficult to verify the fit parameters from the Sharp and Bloomfield fit since the persistence part of the fit cannot be easily separated from the function, as it can for the unified fit of Figure 2. The persistence lengths measured in this work agree with values estimated from rheological properties. A value of 32 Å was obtained independently using viscometry.¹ The estimated characteristic ratio is 39.1 ± 0.5 , reflecting a large degree of local persistence in PHB. Globally, PHB chains are Gaussian and can be adequately described by a Gaussian mass-fractal dimension of 2.

Acknowledgment. G.B. and S.S. were supported in this work by a grant from the Donors of Petroleum Research Fund, Administered by the American Chemical Society (PRF-G). Support of M.S. and S.R. came from Procter & Gamble through the operating budget of Miami Valley Laboratories. PHB and d-PHB were supplied by Procter & Gamble. Special thanks are due to C. Glinka of the National Institute of Standards and Technology for setting up the cryostat for this work. C. C. Han, B. Hammouda, A. Nakatani, and C. Glinka assisted in operating the 8 m SANS line at NIST.

References and Notes

- (1) Satkowski, M. M.; Cornfield, J. S.; Smith, S. Manuscript in preparation, 1997.
- (2) de Koning, G. J. M. Prospects of Bacterial Poly[(R)-3-Hydroxyalkanoates]. Ph.D. Dissertation, University of Eindhoven, The Netherlands, 1993.
- (3) Hocking, P. J.; Marchessault, R. H. Biopolyesters. In Chemistry and Technology of Biodegradable Polymers; Griffin, G. J. L., Ed.; Blackie Academic & Professional Publishers: Glasgow, U.K., 1994.
- (4) Porod, G. *Monatsh. Chem.* **1949**, *80*, 251–255.
- (5) Kratky, O.; Porod, G. *Rec. Trav. Chim. Pays-Bas* **1949**, *68*, 1106–1122.
- (6) Kuhn, W. *Kolloid-Z.* **1934**, *68*, 2–15.
- (7) Benoit, H.; Doty, P. *J. Phys. Chem.* **1953**, *57*, 958–963.
- (8) Doi, M.; Edwards, S. F. *The Theory of Polymer Dynamics*; Oxford Science Publications, Clarendon Press: New York, 1986.
- (9) Degennes, P. *Scaling Concepts in Polymer Physics*; Cornell University Press: Ithaca, NY, 1979.
- (10) See, for example, the chapter by O. Kratky and the chapter by R. G. Kirste and R. C. Oberthur: Glatter, O.; Kratky, O. *Small Angle X-ray Scattering*; Academic Press: New York, 1982.
- (11) See, for example: Feigin, L. A.; Svergun, D. I. *Structure Analysis by Small-Angle X-ray and Neutron Scattering*; Plenum Press: New York, 1987.
- (12) Higgins, J. S.; Benoit, H. C. *Polymers and Neutron Scattering*; Oxford Science Publications: Oxford, U.K., 1994.
- (13) See, for example: Schmidt, P. W. *J. Appl. Crystallogr.* **1992**, *15*, 567–569.
- (14) Flory, P. J. *Statistical Mechanics of Chain Molecules*; Interscience Publishers: New York, 1969.
- (15) Sukumaran, S.; Beaucage, G. Manuscript in preparation, 1997.
- (16) Volkenstein, M. V. *Configurational Statistics of Polymeric Chains*; Interscience: New York, 1963.
- (17) Yoon, D. Y.; Flory, P. J. *Polymer* **1975**, *16*, 645–648.
- (18) Yoon, D. Y.; Flory, P. J. *Macromolecules* **1976**, *9*, 294–299.
- (19) Yoon, D. Y.; Flory, P. J. *Macromolecules* **1976**, *9*, 299–303.
- (20) Wunderlich, W.; Kirste, R. G. *Ber. Bunsen-Ges. Phys. Chem.* **1964**, *68*, 646–652.
- (21) Kirste, R. G. *Makromol. Chem.* **1967**, *101*, 91–103.
- (22) Kirste, R. G. *J. Polym. Sci., Part C* **1967**, *16*, 2039–2048.
- (23) Sharp, P.; Bloomfield, V. A. *Biopolymers* **1968**, *6*, 1201–1211.
- (24) Schmidt, C. W.; Rinehart, F. P.; Hearst, J. E. *Biopolymers* **1971**, *10*, 883–893.
- (25) Debye, P. *J. Phys. Colloid Chem.* **1947**, *51*, 18–32. Technical Report 637 to Rubber Reserve Co., 1945, reprinted in: The Collected Papers of Peter J. W. Debye; Interscience Pub.: New York, 1954.
- (26) Guinier, A.; Fournet, G. *Small-Angle Scattering of X-rays*; John Wiley and Sons: New York, 1955.
- (27) Reviewed in: Daoud, M.; Stanley, H. E.; Stauffer, D. Chapter 6: Scaling Exponents and Fractal Dimensions. In *Physical Properties of Polymers Handbook*; Mark, J. E., Ed.; American Institute of Physics Press: Woodbury, NY, 1996.
- (28) Beaucage, G. *J. Appl. Crystallogr.*, in press.
- (29) Beaucage, G. *J. Appl. Crystallogr.* **1995**, *28*, 717–728.
- (30) Beaucage, G.; Schaefer, D. W. *J. Non-Cryst. Solids* **1994**, *172–174*, 797.
- (31) Beaucage, G.; Ulibarri, T. A.; Black, E.; Schaefer, D. W. In *Organic Hybrid Materials*; Mark, J. E., Lee, C. Y.-C., Bianconi, P. A., Eds.; ACS Symposium Series 585; American Chemical Society: Washington, DC, 1995; p 97.
- (32) Ulibarri, T. A.; Beaucage, G.; Schaefer, D. W.; Olivier, B. J.; Assink, R. A. In *Submicron Multiphase Materials*; Baney, R. H., Gilliom, L. R., Hirano, S., Schmidt, H. K., Eds.; Materials Research Society Symposium Proceedings 274; Materials Research Society: Pittsburgh, PA, 1992; p 85.
- (33) Hua, D. W.; Anderson, J.; Hareid, S.; Smith, D. M.; Beaucage, G. In *Better Ceramics through Chemistry 6*; Cheetham, A. K., Brinker, C. J., Mecartney, M. L., Sanchez, C., Eds.; Materials Research Society Proceedings 346; Materials Research Society: Pittsburgh, PA, 1994; p 985.
- (34) Schaefer, D. W.; Pekala, R.; Beaucage, G., *J. Non-Cryst. Solids* **1995**, *186*, 159–167.
- (35) It should be noted that the high- q limit in the Gaussian regime (first set of brackets) is l_p rather than R_{g1} as has been used for mass-fractal scaling in inorganic materials such as in refs 24, 26, 29, and 30. In these inorganic systems the equivalent of a persistence unit is a 3-D substructure. For the Kratky/Porod chain, the persistence unit is a 1-D structure and only the length of these rodlike units is important to the limitation of the Gaussian power-law regime. If the base unit of the chain were 3-D rather than 1-D, l_p would be replaced by R_{g1} .
- (36) Kurata, M.; Tsunashima, Y. In *Polymer Handbook*, 3rd ed.; John Wiley and Sons: New York, 1989; pp VII/1–3.
- (37) Tsvetkov, V. N.; Andreeva, L. N. In *Polymer Handbook*, 3rd ed.; John Wiley and Sons: New York, 1989; p VII/577.
- (38) Schmitz, K. S. *An Introduction to Dynamic Light Scattering by Macromolecules*; Academic Press: New York, 1990; pp 57–65.
- (39) Flory, P. J. *Principles of Polymer Chemistry*; Cornell University Press: Ithaca, NY, 1953.
- (40) This is consistent with the use of $g_D(q, R_g)$, (2), in the RPA approach of ref 8, which depends only on the global parameter R_g and not n_{chem} .
- (41) Satkowski, M. M.; Doi, Y. Microbial synthesis of d-isotactic PHB. Manuscript in preparation, 1997.
- (42) Shechtman, L. A. Synthesis of Atactic Polyhydroxybutyrate. Manuscript in preparation, 1997.